Nanowire Solar Cells

DOI: 10.1002/anie.200903114

Tantalum-Doped Titanium Dioxide Nanowire Arrays for Dye-Sensitized Solar Cells with High Open-Circuit Voltage**

*Xinjian Feng, Karthik Shankar, Maggie Paulose, and Craig A. Grimes**

Liquid-junction dye-sensitized solar cells (DSSCs) based on nanocrystalline titania (TiO_2) electrodes constitute a potentially low-cost alternative to traditional inorganic silicon-based photovoltaics and have been studied extensively over the past two decades.[1–3] Liquid-junction DSSCs now show high short-circuit photocurrent densities (J_{sc}) and good fill factors (*FF*) owing to improvements made in the photosensitizer and the titania electrodes. Despite these improvements, a remaining issue of critical importance is the relatively low open-circuit photovoltage (V_{oc}) obtained. The V_{oc} of a liquid-junction DSSC is determined by the energy difference between the quasi-Fermi level (QFL) of the semiconductor and the potential of the redox couple in the electrolyte. For n-type TiO_2, the injection of electrons from photoexcited dye molecules raises the QFL towards the conduction band (CB).[4,5] Thus, the maximum achievable V_{oc} would correspond to the case of a degenerate semiconductor and would therefore equal the energy difference between the TiO_2 CB edge and the widely used tri-iodide redox level; this theoretical maximum achievable value of V_{oc} for n-TiO_2-based DSSCs is 0.95 V.[6] Nevertheless, V_{oc} values of 0.7–0.8 V are typically obtained in reported DSSCs, with the deviation from the theoretical maximum commonly explained by interfacial recombination at the TiO_2–dye or TiO_2–electrolyte interfaces. Substantial efforts have been made to improve the photovoltage obtained by retarding the recombination losses. For example, a thin overcoat of different insulting metal oxides, such as Nb_2O_5 and Al_2O_3, have frequently been used to modify the TiO_2 electrode by making a core/shell structure.[7–9] Several kinds of organic molecular additives, such as deoxycholic acid, 4-guanidinobutyric acid, and 4-*tert*-butylpyridine (TBP) have also been used in the redox electrolyte.[10–13] However, these approaches have been found to yield only approximately 50 mV improvement in the open-circuit photovoltage.

The intentional incorporation of atomic impurities into semiconducting materials is a common approach for tailoring properties such as band gap or electric conductivity for specific applications.[14] Doping is routinely performed with bulk semiconductors and has recently been extended to nanoscale materials as well.[15] Among nanostructured materials, semiconducting nanowires are widely studied because of their special electrical and optical properties and because it is possible to use them as components in functional devices such as solar cells.[16,17] Unlike bulk materials, one-dimensional nanowires are usually prepared under non-equilibrium conditions, and it has proved challenging to dope them homogeneously;[18] high-temperature vapor-phase approaches are commonly employed in their synthesis, which are limited in regards to homogeneous doping and alloying because of the high growth temperatures. In contrast, low-temperature hydrothermal synthesis approaches possess an inherent advantage over vapor-phase routes for doping purposes. There have recently been reports on the synthesis of aligned rutile TiO_2 nanowire arrays on transparent conducting oxide (TCO) substrates by hydrothermal synthesis;[17] however, no reports of anisotropic transition-metal-doped TiO_2 nanowires grown on TCO substrates in the solution phase exist.

Herein, we present the synthesis of titania nanowire arrays homogeneously doped with tantalum and prepared under hydrothermal conditions. The synthetic process presented herein should readily be extendable to allow doping of nanowires with different transition metals (e.g., Fe, W, Cr); however, this report is limited to the Ta-doped system. Further, we have translated this advance in materials synthesis into enhanced device performance by demonstrating dye-sensitized solar cells with a very high open-circuit photovoltage of 0.87 V, strikingly close to the theoretical maximum.

Figure 1a,b shows field-emission scanning electron microscopy (FESEM) top-surface images of a typical as-synthesized nanowire array sample at both low and high magnification. A highly uniform and densely packed array of nanowires is obtained, with an average wire width of approximately 20 nm. Figure 1c is a cross-sectional view of the same film with a thickness of approximately 3.6 μm, indicating that the nanowires grow almost perpendicularly from the substrate. This finding is confirmed by the X-ray diffraction (XRD) pattern, which shows a remarkably enhanced (002) peak (Figure 1d). XRD patterns indicate the absence of peaks corresponding to the Ta_2O_5 phase. Owing to the low doping concentration detected by energy-dispersive X-ray spectroscopy (EDX; 0.83 at%) and to the comparable ionic radii of tantalum (0.064 nm) and titanium ions (0.061 nm), no peak shift was detected after tantalum doping. Figure 1e is a high-resolution TEM (HRTEM) image of the as-prepared nanowire sample, showing the nanowires to be highly crystalline (rutile). The nanowires grow in the (001) direction with the [110] crystal plane parallel to the

[*] Dr. X. J. Feng, Dr. K. Shankar, M. Paulose, Prof. C. A. Grimes
Materials Research Institute, The Pennsylvania State University
University Park, PA 16802 (USA)
E-mail: cgrimes@engr.psu.edu
Dr. K. Shankar, Prof. C. A. Grimes
Department of Electrical Engineering, The Pennsylvania State University
University Park, PA 16802 (USA)

[**] This research is supported by the Department of Energy, Grant Number DE-FG36-08GO18074. We thank Trevor Clark at Materials Research Institute of Penn State University for help with the HRTEM and line profile scan experiments and helpful discussion.

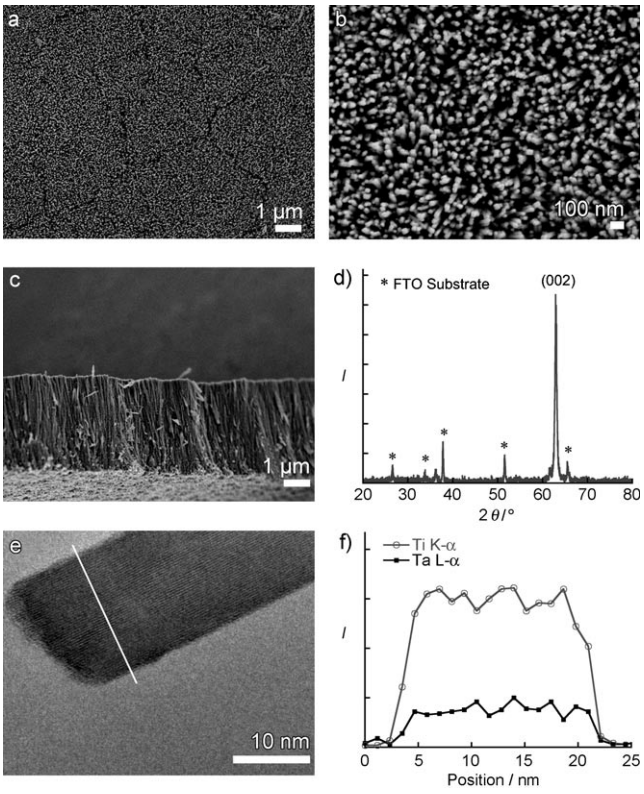

Figure 1. a, b) FESEM top-surface images of the tantalum-doped rutile TiO_2 nanowire array films deposited on TCO substrate at low and high magnification, respectively. c) Cross-sectional FESEM image of the nanowire array films. d) XRD pattern of the as-synthesized Ta-doped nanowire array film. e) High-resolution TEM image of a single nanowire. f) Energy-dispersive spectroscopy element line profiles acquired across the single nanowire shown in Figure 1 e.

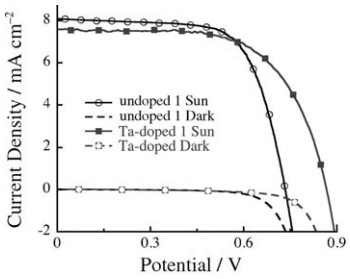

Figure 2. Current–voltage (*J*–*V*) curves for liquid-state DSSCs incorporating Ta-doped and undoped TiO_2 electrodes, measured under simulated AM-1.5 solar illumination at an intensity of 100 mW cm^{-2}. The J_{sc}, *FF*, and efficiency (%) of typical photovoltaic devices were, respectively: for Ta-doped TiO_2 nanowires 7.5 mA, 0.63, and 4.1; for undoped TiO_2 nanowires 8.1 mA. 0.68, and 4.06.

c axis, consistent with the XRD pattern. Unlike traditional methods used to modify TiO_2 electrodes by making an overlayer on the nanocrystals,[7–9] no core/shell structures were found in the present experiment. Figure 1 f shows the energy-dispersive X-ray spectroscopy (EDX) line scan profile acquired across a single nanowire, shown in Figure 1 e, indicating that tantalum doping is homogeneous across the nanowire and that no secondary phase is present.

Solar cells were constructed from Ta-doped and from undoped TiO_2 nanowire arrays. Figure 2 shows *J*–*V* curves of cells made from nanowire arrays. The liquid-state DSSC device using the Ta-doped nanowire array electrode gives a very high photovoltage of 0.87 V. The V_{oc} of DSSCs can be improved by 1) retarding interfacial recombination, 2) shifting the conduction band of TiO_2 to more negative potentials, and 3) engineering a more favorable equilibrium Fermi-level position in TiO_2.[15a] Insulating or wide-band-gap metal oxides have been routinely used to engineer enhancement in DSSC V_{oc} by making a TiO_2/metal oxide core/shell structure.[7–9] Photoexcited dye molecules on the shell tunnel electrons to the core, while the low probability of reverse tunneling from conduction band states and shell-induced passivation of surface states together suppress recombination, resulting in an increased V_{oc}.[19,20] However, in our case, tantalum doping is essentially uniform across the nanowire, and no core/shell structure was found, thus eliminating the possibility of band-gap or carrier concentration gradients inside the nanowires.

Cathodic polarization curves recorded for tantalum-doped and undoped TiO_2 nanowire arrays in the dark are shown in Figure 3 a. The difference in behavior of the curves can be ascribed to a different charge-transfer process for hydrogen evolution and intercalation.[21,22] With negative bias applied to a semiconductor electrode, charge will first fill the empty surface states below the conduction band edge and then become accumulated in the space charge layer. A marked increase in cathodic current (hydrogen evolution/intercalation) will occur when the potential exceeds the flat-band edge in the negative scan direction. The difference in cathodic polarization behaviors indicates that the flat-band edge of tantalum-doped nanowires shifts negatively as compared with an undoped titania sample, which is also confirmed by Mott–Schottky measurement as shown in Figure 3 b. The flat-band potential V_{FB} of nanowire samples with and without Ta doping were determined to be −0.14 and 0.3 V (vs. Ag/AgCl), respectively. This negative movement of

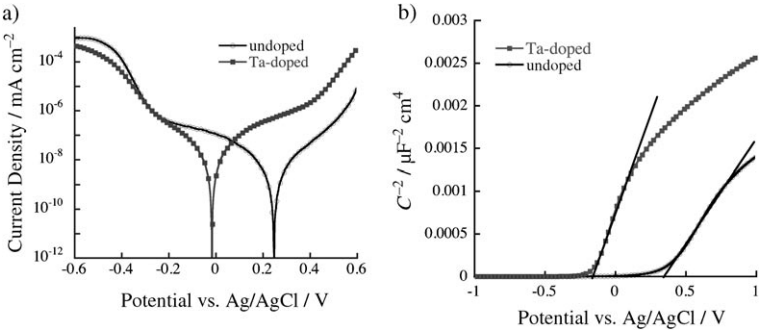

Figure 3. a) Polarization curves of tantalum-doped and undoped TiO_2 nanowire arrays obtained in 0.1 M Na_2SO_4 electrolyte solution. Negative scan speed: 10 mV s^{-1}; b) Mott–Schottky plots for tantalum-doped and undoped TiO_2 nanowire arrays electrode at 298 K in 3 M KCl solution (Ag/AgCl reference electrode).

the flat-band edge can be due to a shift in the position of the conduction band edge of rutile to higher potentials owing to Ta doping. In our case, we do not observe any increase in the band gap for Ta-doped TiO_2. Thus, an upward movement of the CB edge would have to be accompanied by an upward shift in the valence band (VB) edge as well, which is unlikely.

On the other hand, the same shift can also be interpreted as a natural consequence of the modified carrier concentration and trap distribution and the related upward shift in the Fermi level caused by tantalum doping. Owing to the high surface-to-volume ratio of a single nanowire, Fermi-level pinning throughout each nanowire arising from surface defects is possible. Tantalum has a 5^+ valence and an ionic radius similar to that of Ti^{4+}, thus the introduction of tantalum increases the electron concentration.[23] The electrons partially fill the surface traps, leading to an upward shift of the Fermi level. Figure 4 shows the photocurrent density–potential curves of Ta-doped and undoped samples under band-gap illumination; clearly the open-circuit potential of the Ta-doped electrode is negatively shifted by 210 mV compared with the undoped electrode. Taken together, the negative shift in the flat-band potential and open-circuit potential under illumination in Ta-doped nanowires suggests that a higher quasi-Fermi level in the doped electrode may be responsible for the V_{oc} enhancement in DSSCs. Under illumination, fewer photoelectrons are required to completely fill surface states and unpin the Fermi Level in Ta-doped nanowire electrodes. Consequently, for the same level of illumination, a higher quasi-Fermi level closer to the conduction band is achieved, which leads to the larger V_{oc} for liquid-state DSSCs employing Ta-doped TiO_2 nanowire arrays.

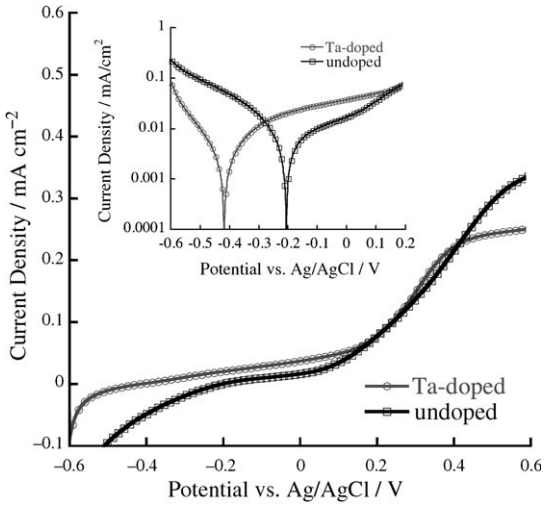

Figure 4. Photocurrent density-applied potential curves for tantalum-doped and undoped TiO_2 nanowire semiconductor photoelectrodes. All data recorded in 0.1 M Na_2SO_4 electrolyte solution under 365 nm UV irradiation. Positive scan speed: 10 mV s^{-1}. The inset is the same curve plotted in log scale.

In conclusion, tantalum-doped TiO_2 nanowire arrays were successfully prepared by a low-temperature hydrothermal method. Doping was homogenous across the nanowire as confirmed by XRD, HRTEM, and the TEM-EDX line profile scan. This method can be used to tune the flat-band potential of nanowire array electrodes. The doping is easily extendable to allow homogeneous doping of other metal cations into Ti^{4+} sites in nanowires, which will be of tremendous use in ultracapacitors, catalysis, and photoelectric conversion applications. Liquid-state DSSCs employing the tantalum-doped TiO_2 nanowire arrays as electrode achieve a very high open-circuit voltage of 0.87 V, close to the theoretical maximum.

Experimental Section

Tantalum-doped TiO_2 nanowire arrays were prepared by a hydrothermal method: Well-cleaned glass substrates coated with fluorine-doped tin oxide (FTO) were dip-coated with peptized TiO_2 solution,[24] dried in an oven at 120 °C, and then heated at 500 °C for 1 h to obtain a layer of TiO_2. This process was repeated twice to obtain a high-quality conformal coating of TiO_2 approximately 30 nm thick, which acted to promote nucleation and prevent electrical contact with the underlying FTO. To grow nanowire arrays, the as-treated FTO substrates were then loaded into a sealed Teflon reactor containing 10 mL toluene, 1 mL titanium tetrachloride (1 M in toluene), 1 mL tetrabutyl titanate, tantalum(V) chloride (1 mol %), and 1 mL hydrochloride acid (37 wt %). A reaction temperature of 160 °C for 10 h was used. After the reaction was completed, the nanowire-covered FTO substrates were carefully washed with ethanol and annealed at 450 °C for 30 min in air to remove the surface-absorbed molecular organic species.

Dye-sensitized solar cells were prepared using the following procedure: Nanowire array samples were coated with dye by immersion overnight in a 0.5 mM solution of commercially available N719 dye. Liquid-junction solar cells were prepared by infiltrating the dye-coated TiO_2 electrode with redox electrolyte containing lithium iodide (LiI, 0.1 M), diiodine (I_2 0.01 M), TBP (0.4 M), butylmethylimidazolium iodide (BMII, 0.6 M), and guanidinium thiocyanate (GuNCS, 0.1 M) in a mixture of acetonitrile and methoxypropionitrile (v/v = 15:1). Conductive glass slides, sputter-coated with 100 nm of Pt, were used as the counter-electrode. Electrode spacing between the nanowire and counter-electrodes was ensured by a 25 μm thick SX-1170 spacer. Photocurrent density and the photovoltage of the dye-sensitized solar cells were measured with active sample areas of 0.8 cm^2 using AM-1.5 simulated sunlight produced by a 50 W Oriel Solar Simulator, calibrated with a NREL-certified silicon solar cell. Mott–Schottky measurements were performed in 3 M KCl at 10 kHz using a Solartron S1287 Electrochemical Interface and 1255B Frequency Response Analyzer (Solartron Analytical, UK), and polarization curves were collected in 0.1 M Na_2SO_4 using a CHI600C potentiostat.

Received: June 9, 2009
Published online: September 18, 2009

Keywords: doping · energy conversion · nanostructures · tantalum · titanium dioxide

[1] B. O'Regan, M. Grätzel, *Nature* **1991**, *353*, 737 – 739.
[2] M. A. Green, K. Emery, Y. Hisikawa, W. Warta, *Prog. Photovoltaics* **2007**, *15*, 425 – 430.
[3] A. Mishra, M. K. R. Fischer, P. Bäuerle, *Angew. Chem.* **2009**, *121*, 2510 – 2536; *Angew. Chem. Int. Ed.* **2009**, *48*, 2474 – 2499.
[4] N. Kopidakis, K. D. Benkstein, J. van de Lagemaat, A. J. Frank, Q. Yuan, E. A. Schiff, *Phys. Rev. B* **2006**, *73*, 045326.
[5] M. Ni, M. K. H. Leung, D. Y. C. Leung, K. Sumathy, *Sol. Energy Mater. Sol. Cells* **2006**, *90*, 2000 – 2009.

[6] a) Y. Ogomi, T. Kato, S. Hayase, *J. Photopolym. Sci. Technol.* **2006**, *19*, 403 – 408; b) strictly speaking, in highly degenerate n-type semiconductors, the Fermi level can be located higher in energy than the conduction band edge.
[7] S. G. Chen, S. Chappel, Y. Diamant, A. Zaban, *Chem. Mater.* **2001**, *13*, 4629 – 4634.
[8] A. Kay, M. Grätzel, *Chem. Mater.* **2002**, *14*, 2930 – 2935.
[9] E. Palomares, J. N. Clifford, S. A. Haque, T. Lutz, J. R. Durrant, *J. Am. Chem. Soc.* **2003**, *125*, 475 – 482.
[10] M. K. Nazeeruddin, A. Kay, I. Rodicio, R. Humphry-Baker, E. Mueller, P. Liska, N. Vlachopoulos, M. Grätzel, *J. Am. Chem. Soc.* **1993**, *115*, 6382 – 6390.
[11] G. Schlichthörl, S. Y. Huang, J. Sprague, A. J. Frank, *J. Phys. Chem. B* **1997**, *101*, 8141 – 8155.
[12] K. Hara, Y. Dan-oh, C. Kasada, Y. Ohga, A. Shinpo, S. Suga, K. Sayama, H. Arakawa, *Langmuir* **2004**, *20*, 4205 – 4210.
[13] Z. P. Zhang, S. M. Zakeeruddin, B. C. O'Regan, R. Humphry-Baker, M. Grätzel, *J. Phys. Chem. B* **2005**, *109*, 21818 – 21824.
[14] a) K. G. Stamplecoskie, J. Ju, S. S. Farvid, P. V. Radovanovic, *Nano Lett.* **2008**, *8*, 2674 – 2681; b) D. E. Perea, E. R. Hemesath, E. J. Schwalbach, J. L. Lensch-Falk, P. W. Voorhees, L. J. Lauhon, *Nat. Nanotechnol.* **2009**, *4*, 315 – 319.
[15] a) R. Jose, V. Thavasi, S. Ramakrishna, *J. Am. Ceram. Soc.* **2009**, *92*, 289 – 301; b) M. Dürr, S. Rosselli, A. Yasuda, G. Nelles, *J. Phys. Chem. B* **2006**, *110*, 21899 – 21902; c) K. Eguchi, H. Koga, K. Sekizawa, K. Sasaki, *J. Ceram. Soc. Jpn.* **2000**, *108*, 1067 – 1071.
[16] A. P. Goodey, S. M. Eichfeld, K. K. Lew, J. M. Redwing, T. E. Mallouk, *J. Am. Chem. Soc.* **2007**, *129*, 12344 – 12345.
[17] a) X. J. Feng, K. Shankar, O. K. Varghese, M. Paulose, T. J. Latempa, C. A. Grimes, *Nano Lett.* **2008**, *8*, 3781 – 3786; b) B. Liu, E. E. Aydil, *J. Am. Chem. Soc.* **2009**, *131*, 3985 – 3990; c) K. Shankar, X. J. Feng, C. A. Grimes, *ACS Nano* **2009**, *3*, 788 – 794.
[18] a) S. C. Erwin, L. J. Zu, M. I. Haftel, T. A. Kennedy, D. J. Norris, *Nature* **2005**, *436*, 91 – 94; b) D. J. Norris, A. L. Efros, S. C. Erwin, *Science* **2008**, *319*, 1776 – 1779.
[19] K. Tennakone, J. Bandara, P. K. M. Bandaranayake, G. R. A. Kumara, A. Konno, *Jpn. J. Appl. Phys.* **2001**, *40*, L732 – L734.
[20] F. Fabregat-Santiago, J. Garcia-Canadas, E. Palomares, J. N. Clifford, S. A. Haque, J. R. Durrant, G. Garcia-Belmonte, J. Bisquert, *J. Appl. Phys.* **2004**, *96*, 6903 – 6907.
[21] A. G. Muñoz, *Electrochim. Acta* **2007**, *52*, 4167 – 4176.
[22] F. Fabregat-Santiago, E. M. Barea, J. Bisquert, G. K. Mor, K. Shankar, C. A. Grimes, *J. Am. Chem. Soc.* **2008**, *130*, 11312 – 11316.
[23] N. Bonini, M. C. Carotta, A. Chiorino, V. Guidi, C. Malagu, G. Martinelli, L. Paglialonga, M. Sacerdoti, *Sens. Actuators B* **2000**, *68*, 274 – 280.
[24] O. K. Varghese, C. A. Grimes, *J. Nanosci. Nanotechnol.* **2003**, 3, 277 – 293.

